

Role of Diffusion in Photoinduced Electron Transfer on a Micelle Surface: Theoretical and Monte Carlo Investigations

Kristin Weidemaier and M. D. Fayer*

Department of Chemistry, Stanford University, Stanford, California 94305

Received: September 18, 1995; In Final Form: November 21, 1995[⊗]

A detailed theoretical treatment of donor–acceptor photoinduced forward electron transfer and back transfer (geminate recombination) for molecules diffusing on a micelle surface is presented. Expressions are given for the time-dependent survival probabilities of both the excited-state donor and the charge-transfer state formed by forward electron transfer. Incorporation of diffusion has a pronounced effect on the kinetics of both the forward and the back transfer, and the amount of geminate recombination depends critically on the Coulombic potential between the ions. Ion spatial distributions as a function of time are presented and used to discuss the possibility of achieving long-term ion separation. The validity of the theory is demonstrated by comparison to Monte Carlo simulations of the problem, and the perfect agreement obtained confirms the accuracy of the theoretical derivation.

I. Introduction

The investigation of reaction dynamics in restricted geometries such as micelles, zeolites, emulsions, and thin films has been the subject of a great deal of recent experimental and theoretical work.^{1–6} The unique spatial arrangement of such systems can give rise to novel chemical behavior in which the dynamics of a given process are sharply influenced by the system topography. It is hoped that research aimed at understanding the relationship between system geometry and reaction rates will ultimately lead to an ability to control the kinetics by manipulating the microscopic environment. Progress in this area has already been observed in the field of catalysis.^{7–11}

An important example of reaction dynamics in restricted geometries is that of photoinduced electron transfer. Ions formed by electron transfer from a photoexcited donor molecule experience a thermodynamic driving force that tends to cause them to recombine, with no net chemical reaction. The interest in electron transfer in restricted geometries stems from the recognition that controlling the topography of the system may hinder the back-transfer reaction, thereby promoting ion separation and potential energy storage. The ability of system geometry to influence the kinetics of both forward and back electron transfer is amply illustrated by photosynthesis, where a precise spatial arrangement of electron donors and acceptors provides efficient charge separation.^{12,13}

Recent work on electron-transfer systems has tended to fall loosely into one of two categories. In the first, inter- or intramolecular electron-transfer systems are designed with a single, fixed separation distance between the donor and acceptor. By varying the separation distance, the nature of the separating medium, and the character of the donors and acceptors themselves, valuable information about the reaction rate is obtained.^{14–21} More recently, however, there has been interest in a second category of intermolecular electron-transfer systems.^{22–34} For systems of this type, a number of acceptors may exist in a complicated spatial array about the donor. In such circumstances, there is no longer one characteristic distance for the problem, but electron transfer can occur through solvent to any of a number of acceptors. Determining which acceptor receives the electron requires a detailed knowledge of the full

distance dependence of the electron-transfer rate. Moreover, the back-transfer process is coupled to the forward transfer in a complex fashion. A macroscopic system will consist of an ensemble of possible donors, each surrounded by its own unique configuration of acceptors. Where the ions are formed is determined by the distribution of forward-transfer pathways. The back-transfer dynamics, then, depend on the spatial distribution of ions formed by the forward transfer, and the survival time of the ions is thus coupled to the forward-transfer kinetics in a nontrivial way. The complexities of the ensemble averaging techniques involved in handling a problem of this sort have led to various approximations to simplify the full spatial dependence of the back-transfer process.^{32,35,36} Many of these approximations have been shown to be highly inaccurate at anything other than very low acceptor concentrations.^{37,38}

Recently, a rigorous theoretical treatment has been developed for photoinduced electron transfer in isotropic three dimensions.^{24,29,30,39,40} The theory properly performs the full set of ensemble averages for both the forward- and back-electron-transfer processes and permits calculation of the time-dependent survival probabilities of the excited-state donor and the ions formed by electron transfer. This theoretical treatment has been extended to describe electron transfer in liquids where the diffusion of donors and acceptors dramatically affects the kinetics of the forward- and back-transfer reactions.^{24,29,30,40}

For electron transfer in a restricted geometry, the static problem has recently been solved.³⁸ In this article, we extend this treatment to include the effects of diffusion. Specifically, we concentrate on photoinduced electron transfer occurring on a micelle surface where the particles are free to diffuse over the surface of the micelle. This problem is of interest for two reasons. First, this is the first complete description of forward and back electron transfer between a donor and a number of competing acceptors in a restricted geometry where diffusion of the particles is included. We note that the results are particularly relevant for the analysis of experimental data. For example, recent experiments have studied electronic excitation transport among chromophores on micelles.^{41,42} Analogous experiments could be performed for chromophores that undergo electron transfer, and the results will depend critically on whether the chromophores diffuse significantly on the time scale of the electron-transfer events. Importantly, experimental

[⊗] Abstract published in *Advance ACS Abstracts*, February 1, 1996.

measurements of diffusion constants for chromophores in micelles have shown that these diffusion constants can be significant.⁴² The second reason for the usefulness of this work is that, although this paper is concerned with electron transfer, the methods developed here to treat diffusion in the restricted geometry of a micelle surface can be extended to include other types of reactions in other geometries, albeit with varying levels of mathematical complexity.

The theoretical methods presented here involve sets of ensemble averages over all possible configurations of acceptors about the donor. To verify the accuracy of the theory, we also report Monte Carlo simulations of electron transfer on the surface of a micelle. Diffusion of the particles over the surface of the micelle is included in the Monte Carlo simulations, and comparisons of the simulation and theoretical results show perfect agreement.

II. The Model

A detailed description of the electron-transfer system model has been given elsewhere.^{23,38,43} In brief, following photoexcitation, an excited electron donor can either relax to the ground state or can transfer an electron to one of the available surrounding acceptors. The electron-transfer process will result in the formation of radical ions, with charges determined by their initial pretransfer charges. An initially neutral donor and acceptor will result in the formation of a cation and anion which will experience a strong Coulombic attraction. In a diffusing system, the Coulombic attraction will significantly affect the charge-recombination dynamics. Analogously, a neutral donor with a positively charged acceptor or a neutral donor with a doubly positive acceptor will give rise to ions that experience no Coulombic interaction or a repulsive one, respectively. Note that for the three cases just mentioned, there is no Coulombic interaction between the donors and acceptors prior to the forward-transfer event. In such cases, the initial distribution of acceptors about the donor can be assumed to be random. Although more complicated initial distributions can be readily included in the theory, here we consider only random starting configurations in order to simplify the analysis. Following the forward-transfer event, the ions created can either back-transfer, thereby regenerating the ground state, or undergo diffusive motion that (perhaps aided by Coulombic repulsion) can result in long-term ion separation. In this model, following forward electron transfer, further electron transfer is only geminate, returning the electron to the original donor. The possibility of the electron hopping from one acceptor to another is excluded. This is physically reasonable for many systems, as has been discussed recently,⁴³ since there is no thermodynamic driving force for acceptor-acceptor transfer, while geminate recombination is usually substantially downhill. However, this is an approximation, and in some systems, acceptor-acceptor electron hopping could play a role that is not included in the model.

The restricted geometry system modeled here is one in which electron transfer occurs between particles constrained to lie on the surface of a micelle. The micelle is modeled as a sphere of radius R , and the donor and acceptors are taken to be curved disks on the surface of the sphere, with curvature matching that of the micelle. (See Figure 1.) The coordinate frame is chosen so that the donor is always at the north pole, with the donor-acceptor distance given by the polar angle θ . Diffusion of the donor and acceptors over the surface of the micelle is permitted and is characterized by the relative diffusion constant, $D = D_d + D_a$, where D_d and D_a are the lateral diffusion constants of the donor and acceptor, respectively. For a many-body problem, a coordinate transform of this type is not exact, since the motion

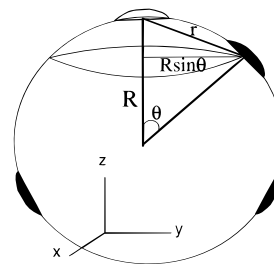


Figure 1. Pictorial representation of the micelle system along with the coordinate frame used in section III. The donor and acceptors exist as curved disks on the surface of the micelle, with radius of curvature matching that of the micelle. (Donor shown as the unfilled disk and acceptors as solid-filled disks.) The relevant electron-transfer distance is the through-sphere distance or chord length, r , related to the angular distance θ by $r = 2R \sin(\theta/2)$.

of the particles is coupled by virtue of the fact that motion of the donor toward any one acceptor necessarily implies motion away from some other acceptor in the system. Treating the diffusion of the particles by the relative diffusion constant $D = D_d + D_a$, however, has been shown to be essentially perfect.⁴³

The concentration of electron donors is much less than that of the acceptors. For sufficiently low donor concentrations, on average, only one donor will exist on the surface of any given micelle, and this donor may transfer to any of the N acceptors on the same micelle. (See Figure 1.) The relevant electron-transfer distance is the through-sphere, or chord, distance. The micelle concentration is taken to be low so that Förster energy transfer between donors on two different micelles is insignificant and so that electron transfer between a donor on one micelle and an acceptor on another does not occur. In accordance with experimental evidence,⁴² the diffusion of the micelles themselves is much slower than that of the donors and acceptors so that the micelle can be taken to be static on the time scale of the relevant electron-transfer events.

The set of assumptions given above, although they simplify the problem, are nevertheless experimentally realistic. Given the often steep distance dependence of the forward reaction, electron transfer between donors and acceptors will be the dominant kinetic event, as the low-concentration donors transfer to the surrounding, much higher concentration of acceptors. Real molecules will have finite sizes that influence the transfer kinetics. The primary effect is that of donor-acceptor excluded volume, since the donor and acceptor cannot approach closer than the sum of their radii. This is readily included in the theory by incorporating a cutoff in the spatial integrals. The role of acceptor-acceptor excluded volume is more subtle and has been shown to be insignificant at all but the highest acceptor concentrations.^{38,44}

III. Theory

A. Forward Transfer. The theoretical quantities of interest are the survival probabilities of the excited donor and the charge-transfer products, $\langle P_{\text{ex}}(t) \rangle$ and $\langle P_{\text{ct}}(t) \rangle$, where $\langle P_{\text{ex}}(t) \rangle$ is the probability that a donor excited at time $t = 0$ is still excited at some later time t and $\langle P_{\text{ct}}(t) \rangle$ is the probability that an ion formed by charge transfer still exists at time t . The brackets denote that the survival probabilities are the ensemble averaged ones. The starting point in the derivation is writing the differential equations for the special case of one donor and only one acceptor. For the forward transfer, the relevant equation is

$$\frac{\partial}{\partial t} S_{\text{ex}}(t|\theta_0) = D \nabla_{\theta_0}^2 S_{\text{ex}}(t|\theta_0) - k_{\text{f}}(\theta_0) S_{\text{ex}}(t|\theta_0) \quad (1)$$

Here, $S_{\text{ex}}(t|\theta_0)$ is the probability that, if the donor is excited at $t = 0$ with the acceptor located at θ_0 , then the donor is still excited at some later time t . Note that during this time interval, the acceptor may have diffused to some other position in the system. $\nabla_{\theta_0}^2$ is the relevant component of the Laplacian for motion along the surface of a sphere. Examination of Figure 1 shows that the donor-acceptor distance is completely characterized by the angle θ_0 , and thus, only the polar component of the Laplacian is needed. This is

$$\nabla_{\theta_0}^2 = \frac{1}{R \sin \theta_0} \frac{\partial}{\partial \theta_0} \left[\frac{\sin \theta_0}{R} \frac{\partial}{\partial \theta_0} \right] \quad (2)$$

where R is the micelle radius and θ_0 is the acceptor's initial position in a coordinate system with the donor at the north pole. In eq 1, $k_f(\theta_0)$ is the rate constant for the forward-transfer process and depends on the distance between the donor and acceptor (θ_0). The distance dependence of the rate constant can be of any form, but here we assume the widely-accepted Marcus form:^{45,46}

$$k_f(\theta_0) = \frac{2\pi}{\hbar} J_{\text{of}}^2 \exp[-2R\beta_f(\sin(\theta_0/2) - \sin(\theta_c/2))] \frac{1}{\sqrt{4\pi\lambda k_B T}} \exp\left[\frac{-(\Delta G_f + \lambda)^2}{4\lambda k_B T}\right] \quad (3)$$

where

$$\lambda = \frac{e^2}{2} \left(\frac{1}{\epsilon_{\text{op}}} - \frac{1}{\epsilon_s} \right) \left(\frac{1}{r_d} + \frac{1}{r_a} - \frac{1}{R \sin(\theta_0/2)} \right)$$

Here, ϵ_{op} and ϵ_s are the high-frequency and static dielectric constants, respectively, which may vary directionally inside and along the micelle. r_d and r_a are the half-arc length of the donor and acceptor, respectively, and e is the unit of fundamental charge. In eq 3, ΔG_f is the free-energy change due to the forward transfer, θ_c is the donor-acceptor contact distance in angular units, and \hbar and k_B are the usual Planck's and Boltzmann's constants. J_{of} and β_f are parameters that characterize the magnitude and distance scale of the transfer process. Note that although the relevant electron-transfer distance is the through-sphere distance r , the rate constant is expressed in terms of the angular donor-acceptor separation distance for consistency with eqs 1 and 2. The two quantities are related by $r = 2R \sin(\theta_0/2)$. The reason that the initial coordinate θ_0 appears in eqs 1-3 is that the differential equation for $S_{\text{ex}}(t|\theta_0)$ is formally derived by taking the adjoint of the full Green's function for the problem.^{24,39} Equation 1 has associated initial and boundary conditions given by

$$S_{\text{ex}}(0|\theta_0) = 1 \quad (4)$$

$$\frac{\partial}{\partial \theta_0} S_{\text{ex}}(t|\theta_0)|_{\theta_0=\theta_c} = 0 \quad (5)$$

Equation 5 is a reflecting boundary condition at the contact distance between the donor and acceptor, θ_c .

The excited-state survival probability when all N acceptors are present is given by

$$\frac{\partial}{\partial t} P_{\text{ex}}(\theta_1 \dots \theta_N, t | \theta_{01} \dots \theta_{0N}) = \sum_{j=1}^N [D \nabla_{\theta_j}^2 - k_f(\theta_j)] P_{\text{ex}}(\theta_1 \dots \theta_N, t | \theta_{01} \dots \theta_{0N}) \quad (6)$$

If eq 6 is integrated first over all θ_j and then over all θ_{j0} , it can be shown that^{24,39,40}

$$\langle P_{\text{ex}}(t) \rangle = \left[\int_{\theta_c}^{\pi} S_{\text{ex}}(t|\theta) \frac{\sin \theta}{2} d\theta \right]^N \quad (7)$$

In eq 7, θ_c is the donor-acceptor angular contact distance, N is the number of acceptors, and the subscript has been dropped for convenience. Note that in a restricted geometry problem of this type, the number of acceptors N is finite, and the thermodynamic limit of (7) cannot be taken. Equation 7 is written in the absence of donor excited-state fluorescence to emphasize the kinetics of the electron-transfer process. Excited-state donor fluorescence decay would appear as a multiplicative factor $\exp(-t/\tau)$ in eq 7, where τ is the excited-state lifetime.

Equation 1 for $S_{\text{ex}}(t|\theta_0)$ cannot be solved analytically, and numerical evaluation of $S_{\text{ex}}(t|\theta_0)$ must be followed by numerical integration as indicated in eq 7 to give $\langle P_{\text{ex}}(t) \rangle$.

B. Back Transfer (Forward Transfer with Geminate Recombination). Solving for the charge-transfer ion survival probability, $\langle P_{\text{ct}}(t) \rangle$, is substantially more difficult because the kinetics of the back transfer are coupled to those of the forward. The survival probability for the case of one donor and one acceptor is written in a manner analogous to the forward-transfer problem:

$$\frac{\partial}{\partial t} S_{\text{ct}}(t|\theta_0) = L_{\theta_0}^* S_{\text{ct}}(t|\theta_0) - k_b(\theta_0) S_{\text{ct}}(t|\theta_0) \quad (8)$$

$$S_{\text{ct}}(0|\theta_0) = 1 \quad (9)$$

$$\frac{\partial}{\partial \theta_0} S_{\text{ct}}(t|\theta_0)|_{\theta_0=\theta_c} = 0 \quad (10)$$

Here, $S_{\text{ct}}(t|\theta_0)$ is the probability of finding the donor in its ion (charge transfer) state at time t , given that the acceptor was initially located at θ_0 . $L_{\theta_0}^*$ is the adjoint of the Smoluchowski operator which includes the potential between the ions and is given by^{23,47}

$$L_{\theta_0}^* = \frac{D}{R \sin \theta_0} e^{V(\theta_0)} \frac{\partial}{\partial \theta_0} \frac{\sin \theta_0}{R} e^{-V(\theta_0)} \frac{\partial}{\partial \theta_0} \quad (11)$$

where $V(\theta_0)$ is the Coulombic potential between donor and acceptor ions separated by angular distance θ_0 . $k_b(\theta_0)$ is the rate constant for the back-transfer process and is given by eq 3, only with J_{of} , β_f , and ΔG_f replaced by J_{ob} , β_b , and ΔG_b , the relevant parameters for the back transfer. The charge transfer survival probability for any given configuration of all N acceptors is given by

$$\frac{\partial}{\partial t} P_{\text{ct}}^i(\theta_1 \dots \theta_N, t | \theta_{01} \dots \theta_{0N}) = \sum_{j=1}^N L_{\theta_j} P_{\text{ct}}^i(\theta_1 \dots \theta_N, t | \theta_{01} \dots \theta_{0N}) - k_b(\theta_i) P_{\text{ct}}^i(\theta_1 \dots \theta_N, t | \theta_{01} \dots \theta_{0N}) + k_f(\theta_i) P_{\text{ct}}^i(\theta_1 \dots \theta_N, t | \theta_{01} \dots \theta_{0N}) \quad (12)$$

where $P_{\text{ct}}^i(\theta_1 \dots \theta_N, t | \theta_{01} \dots \theta_{0N})$ is the probability that, at time t , the i th acceptor has the electron with the N acceptors located at $\theta_1 \dots \theta_N$ for the initial configuration $\theta_{01} \dots \theta_{0N}$. A technique for solving for $\langle P_{\text{ct}}(t) \rangle$ was developed by Lin *et al.*^{24,39,40} and involves first ensemble averaging eq 12 over the coordinates of the $N - 1$ acceptors without the electron. We quote only the end result from following an analogous procedure for the micelle case:

$$\langle P_{\text{ct}}(t) \rangle = N \int_{\theta_c}^{\pi} \int_0^t S_{\text{ct}}(t - t' | \theta_0) k_f(\theta_0) S_{\text{ex}}(t' | \theta_0) \times \left[\int_{\theta_c}^{\pi} S_{\text{ex}}(t' | \theta_0) \frac{\sin \theta_0}{2} d\theta_0 \right]^{N-1} dt' \frac{\sin \theta_0}{2} d\theta_0 \quad (13)$$

Equation 13 deviates from previously reported results for ion survival probabilities in infinite liquid systems²² in two respects. First, the spatial averaging must be appropriate for the restricted geometry. For particles on the surface of a micelle, the appropriate spatial distribution for the probability of finding a particle at θ_0 is $1/2 \sin \theta_0 d\theta_0$.^{38,48} Second, the term in brackets in eq 13 does not appear in the analogous equation for infinite liquid systems. In infinite systems, the bracketed term in eq 13 becomes simply $\langle P_{\text{ex}}(t) \rangle$ in the thermodynamic limit. For the micelle problem, the thermodynamic limit of eq 13 cannot be taken because of the finite number of acceptors in the restricted geometry.

IV. Numerical Methods and Monte Carlo Simulations

Equations 1 and 8 given above were solved numerically using the Crank–Nicholson algorithm⁴⁹ and a partial differencing scheme suggested by Agmon *et al.*^{50,51} $\langle P_{\text{ex}}(t) \rangle$ and $\langle P_{\text{ct}}(t) \rangle$ were then calculated from eqs 7 and 13 via numerical integration. We wish to stress that obtaining convergence in the solutions of 1 and 8 can be extremely difficult. However, for the vast majority of parameters, step sizes of 0.005 ns in time and 0.002 rad in space proved sufficient.

The full details of the Monte Carlo simulations have appeared elsewhere.^{38,44} In brief, a random configuration of N acceptors about a donor was generated appropriately.^{38,48} The N acceptors were then allowed to diffuse, with each acceptor stepping a distance of $\sqrt{4D\Delta t}$, where $D = D_d + D_a$ is the sum of the donor and acceptor diffusion constants and Δt is the simulation time step. A step size of $\sqrt{4D\Delta t}$ is the result from diffusion in an infinite plane, but for sufficiently small time steps, it is the limiting behavior for diffusion on a sphere. After each time step in the simulation, the probability of forward transfer was calculated from $1 - \exp[-(\sum_j k_f(\theta_j)\Delta t)]$. If forward transfer occurred, then the acceptor receiving the electron was determined, with the probability of the i th acceptor becoming the ion given by $k_f(\theta_i)/\sum_j k_f(\theta_j)$.⁴³ Following forward transfer, the back transfer was simulated by following the motion of the acceptor with the electron. (For the problem in the absence of acceptor–acceptor excluded volume, the other $N - 1$ acceptors do not influence the back-transfer event.) The acceptor with the electron was moved in the appropriate Coulomb potential according to standard Metropolis Monte Carlo techniques,^{52,53} and the probability of back transfer after each diffusion step was calculated as $1 - \exp[-k_b(\theta)\Delta t]$, where θ is the angular distance between the donor and acceptor ions at that time step.

All numerical integration and computer Monte Carlo simulations were performed on an IBM RS6000 Model 3BT workstation. Theoretical calculations of the observables $\langle P_{\text{ex}}(t) \rangle$ and $\langle P_{\text{ct}}(t) \rangle$ from eqs 1, 7, 8, and 13 took between several seconds and a few minutes, while the Monte Carlo simulations required 5–12 h. Hence, the theoretical results presented here represent a tremendous gain in computational efficiency over the simulations.

V. Results and Discussion

Figures 2 and 3 present, respectively, $\langle P_{\text{ex}}(t) \rangle$ (excited-state ensemble averaged survival probability) and $\langle P_{\text{ct}}(t) \rangle$ (charge-transfer-state ensemble averaged survival probability) curves for a variety of electron-transfer parameters. The parameters are given in the figure captions and were chosen to give rate constants with a range of magnitudes and distance dependences. J and β values were selected to correspond with parameters reported in experimental studies of intermolecular electron transfer.^{26,33} Free-energy values are consistent with what might

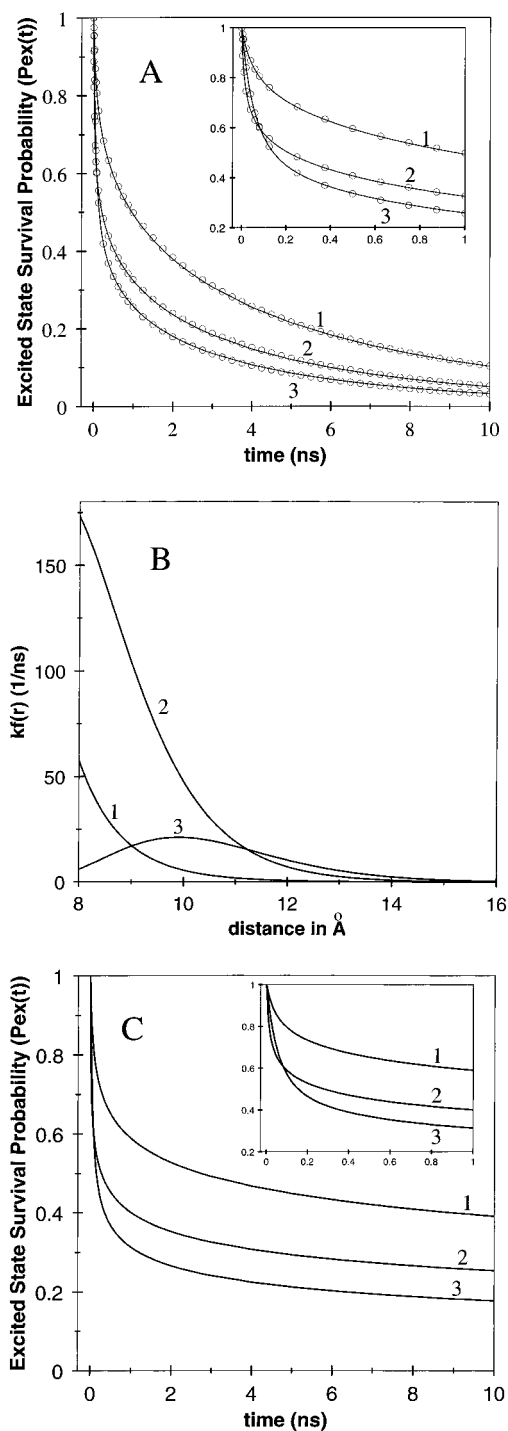


Figure 2. Theoretical and simulated $\langle P_{\text{ex}}(t) \rangle$ curves for three different parameter sets. The open circles are the Monte Carlo simulation results, and the solid lines are the theory. A shows the $\langle P_{\text{ex}}(t) \rangle$ curves for a diffusion constant of $10 \text{ \AA}^2/\text{ns}$, while C shows these same curves for the static problem ($D = 0$). The center panel, B, gives the rate constants as a function of chord distance, r . The numbering of the curves is consistent in all the panels and corresponds to the three parameter sets as follows. Parameter set 1: $J_f = 20 \text{ cm}^{-1}$, $\beta_f = 0.7 \text{ \AA}^{-1}$, $\Delta G_f = -0.5 \text{ eV}$, $J_b = 600 \text{ cm}^{-1}$, $\beta_b = 1.1 \text{ \AA}^{-1}$, $\Delta G_b = -2.0 \text{ eV}$. Parameter set 2: $J_f = 40 \text{ cm}^{-1}$, $\beta_f = 1.0 \text{ \AA}^{-1}$, $\Delta G_f = -1.0 \text{ eV}$, $J_b = 100 \text{ cm}^{-1}$, $\beta_b = 1.0 \text{ \AA}^{-1}$, $\Delta G_b = -1.5 \text{ eV}$. Parameter set 3: $J_f = 240 \text{ cm}^{-1}$, $\beta_f = 1.1 \text{ \AA}^{-1}$, $\Delta G_f = -1.5 \text{ eV}$, $J_b = 20 \text{ cm}^{-1}$, $\beta_b = 0.7 \text{ \AA}^{-1}$, $\Delta G_b = -1.0 \text{ eV}$. All curves were calculated for nine acceptors on a 20-\AA radius micelle with a donor–acceptor contact distance of 8 \AA and optical and static dielectric constants of 2.0 and 10.0, respectively. The $\langle P_{\text{ex}}(t) \rangle$ curves in A and C are shown without donor fluorescence decay in order to emphasize the electron-transfer event. Insets show the short-time behavior.

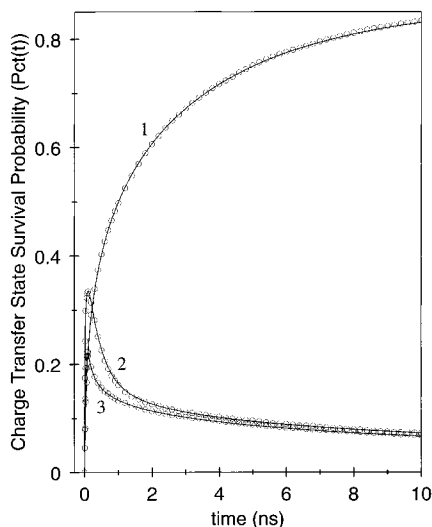


Figure 3. Theoretical and simulated charge-transfer survival probability $\langle P_{ct}(t) \rangle$ curves for the three parameter sets given in the caption to Figure 2. The circles are the Monte Carlo simulations, and the lines are the theory. All three curves are calculated for an Onsager length of 0, *i.e.*, for no Coulombic potential between the donor and acceptor ions, and donor fluorescence lifetime is not included. As for the $\langle P_{ex}(t) \rangle$ curves in Figure 2, agreement between theory and simulation is perfect.

be expected from solutions of the Rehm–Weller equation for aromatic molecules, using visible excitation and typical electrochemical data.^{54,55} Figures 2 and 3 show both theoretical and simulated results, with the simulation given by open circles and the theory by solid lines. As can be seen, the agreement is perfect, confirming the validity of eqs 7 and 13. Theory and Monte Carlo simulations have been compared for a wide variety of electron-transfer parameters, diffusion constants, Onsager lengths, and acceptor numbers. In all cases, excellent agreement was obtained. This is the first time that forward electron transfer with geminate recombination has been treated for molecules diffusing in a restricted geometry, finite volume system. While these results are for the spherical micelle problem, the method used to obtain them is general and can be applied to any restricted geometry system.

The panels in Figure 2 show how the amount of forward transfer depends critically on both the magnitude and distance dependence of the forward-transfer rate. The center panel (Figure 2B) shows the rate constants $k_f(r)$ for the three curves plotted against chord length in Å for ease of discussion. The top panel (2A) shows the $\langle P_{ex}(t) \rangle$ curves for a diffusion constant of $10 \text{ \AA}^2/\text{ns}$, while the bottom panel (2C) shows these same $\langle P_{ex}(t) \rangle$ curves in the absence of diffusion. Of the three curves (labeled 1, 2, and 3 to correspond to the different parameter sets 1, 2, and 3 given in the caption), only curve 3 has a ΔG value sufficiently negative to put its $k_f(r)$ in the Marcus inverted regime. Whereas plots of $k_f(r)$ for curves 1 and 2 show a more-or-less exponential decay with distance, $k_f(r)$ for curve 3 is bell shaped, with a maximum that occurs 2 \AA beyond the contact length. As Figure 2A shows, it is this inverted $k_f(r)$ that leads to the greatest amount of forward electron transfer. This result is unexpected, since $k_f(r)$ for parameter set 2 is substantially larger than $k_f(r)$ for parameter set 3 at all short distances. It is only at distances beyond about 11.5 \AA that the inverted rate constant becomes greater than the noninverted one. (Compare curves 2 and 3 in Figure 2B). This result can be explained as follows. For distances from contact out to 11.5 \AA , $k_f(r)$ for parameter set 2 has values ranging from 175 to 15 ns^{-1} , while the inverted $k_f(r)$ magnitude is everywhere less than 20 ns^{-1} . A value of 20 ns^{-1} , however, still results in large amounts of electron transfer. In fact, if $k_f(r)$ for curve 2 were artificially

capped at 20 ns^{-1} , the resulting $\langle P_{ex}(t) \rangle$ curve would look nearly identical to the $\langle P_{ex}(t) \rangle$ curve for the full (very large) form of the rate constant. This indicates that, for this particular micelle size and number of acceptors, a rate constant of 20 ns^{-1} is sufficient to essentially ensure forward electron transfer from any donor that has an acceptor available within the first few angstroms. The difference between $\langle P_{ex}(t) \rangle$ curves 2 and 3, then, is caused by those subensembles of donors that do **not** have an acceptor available within the first few angstroms. For these subensembles, the probability of forward transfer will be greater for the inverted parameters. This fact, combined with the greater availability of acceptors at larger distances, causes $\langle P_{ex}(t) \rangle$ curve 3 to decay faster than $\langle P_{ex}(t) \rangle$ curve 2.

Figure 2C shows $\langle P_{ex}(t) \rangle$ curves for the same forward-transfer parameters but calculated in the absence of diffusion. There are two points to note. First, the ability of acceptors to diffuse over the surface of the micelle leads to a substantial increase in the amount of forward transfer. Second, the differences between curves 1–3 are accentuated in the static problem. From the plot of rate constants in Figure 2B, it is seen that $k_f(r)$ for parameter set 3 becomes greater than the rate constants for parameter sets 1 and 2 at around 11.5 \AA . As discussed, the fast decay of $\langle P_{ex}(t) \rangle$ curve 3 is due to additional electron transfer to acceptors at these large distances. When diffusion of the acceptors can occur, however, the advantage gained by a donor able to transfer to large distances becomes less significant, since acceptors can move in toward a region of higher reactivity.

The $\langle P_{ct}(t) \rangle$ curves shown in Figure 3 result from the complex coupling between the forward- and back-transfer processes. Since $\langle P_{ex}(t) \rangle$ for curve 3 decays fastest, the overall number of ions formed must be greatest for this set of parameters. However, the $\langle P_{ct}(t) \rangle$ curve corresponding to these forward-transfer parameters decays fastest and is lowest in magnitude because the back-transfer rate is fast at almost every distance where forward transfer is significant. To survive any length of time, an ion would need to diffuse out of the spatial region where $k_b(r)$ is large. For a diffusion constant of $10 \text{ \AA}^2/\text{ns}$, few ions succeed in doing this. Curve 1 in Figure 3 is the only one in which a large fraction of the ions formed by forward transfer survives. This is primarily because the ΔG value for the back transfer is so negative ($\Delta G = 2.0$) and the back transfer is so steeply inverted that $k_b(r)$ is extremely small at all distances. Although this is consistent with the predictions of classical Marcus theory, we note that, for very large negative ΔG values, classical Marcus theory may require quantum mechanical corrections to account for the presence of additional reaction pathways, *i.e.*, tunneling.^{17,19,20}

The curves shown in Figures 2 and 3 are for representative parameters. Different parameter sets can lead to different types of observed behavior, especially in the back transfer. The observed results depend in a complex way on the details of the distance dependence.

Figure 4 shows the pronounced effect of diffusion on the forward- and back-electron-transfer processes. The excited-state and charge-transfer-state (ion) survival probabilities were calculated in the absence of diffusion and then compared to those for $D = 10, 20,$ and $30 \text{ \AA}^2/\text{ns}$. Experimental measurements of the diffusion constant of octadecylrhodamine B and merocyanine 540 in Triton X-100 resulted in numbers in this range.⁴² For all parameter sets studied, diffusion led to a dramatic increase in the amount of forward transfer, since acceptors that begin removed from the donor can diffuse in and react. Of course, acceptors that are close to the donor can diffuse *out* of the region of forward transfer, but for any reasonably fast set of forward-transfer parameters, acceptors

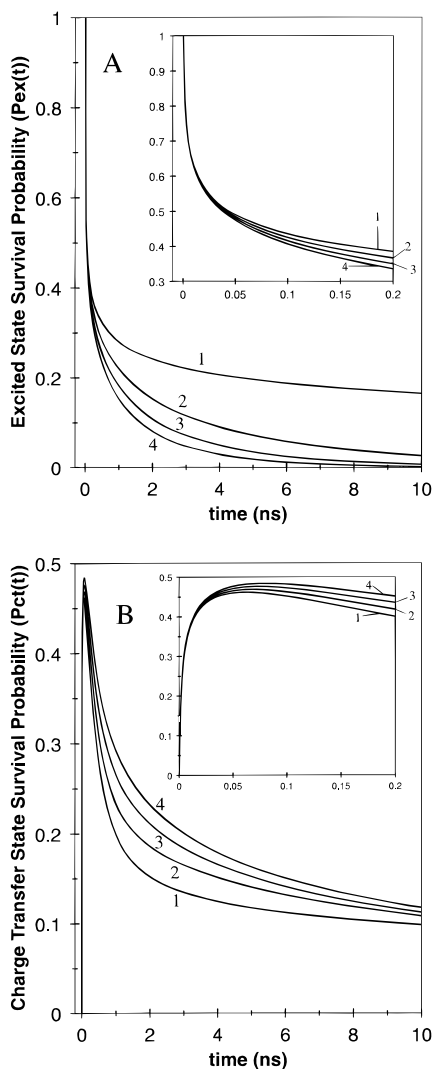


Figure 4. Excited-state ($\langle P_{\text{ex}}(t) \rangle$) and charge-transfer ($\langle P_{\text{ct}}(t) \rangle$) survival probabilities for diffusion constants of 0, 10, 20, and 30 $\text{\AA}^2/\text{ns}$ for curves 1–4, respectively. Insets show short-time behavior for times less than 200 ps. The curves are from the theory (eqs 7 and 13) and do not include donor fluorescence lifetime. The electron-transfer parameters for all curves are $J_f = 100 \text{ cm}^{-1}$, $\beta_f = 1.0 \text{ \AA}^{-1}$, $\Delta G_f = -1.0 \text{ eV}$, $J_b = 100 \text{ cm}^{-1}$, $\beta_b = 1.0 \text{ \AA}^{-1}$, and $\Delta G_b = -1.5 \text{ eV}$. The micelle radius, number of acceptors, and optical and static dielectric constants were $R = 20 \text{ \AA}$, $N = 9$, $\epsilon_{\text{op}} = 2.0$, and $\epsilon_s = 10.0$, and the donor-acceptor contact distance was 8 \AA . No Coulombic potential was included in the back-transfer calculations.

“escaping” from the reacting region are outnumbered by acceptors diffusing in and reacting. Note that because of the generally steep distance dependence of the $k_f(r)$ curves, diffusion over even a small distance can result in a dramatic change in the electron-transfer rate.

Diffusion also significantly affects the $\langle P_{\text{ct}}(t) \rangle$ curves, as seen in Figure 4B. However, the effects are more complex. Because the back-transfer process depends critically on the ion distribution created by forward transfer, the ion survival probability is determined by the interplay between the initial ion distribution, the ion diffusion constant, and the form of the back-transfer rate. For the parameter sets shown in Figure 4B, diffusion of the ions leads to an enhanced escape probability. This, however, is not general, and for different parameter sets, diffusion may actually lead to a decrease in the ion survival probability. This is commonly observed when the back transfer is inverted so that the back-transfer rate is peaked several angstroms out from contact. Forward transfer can then create an initial distribution of ions centered about a region where the back-transfer rate is

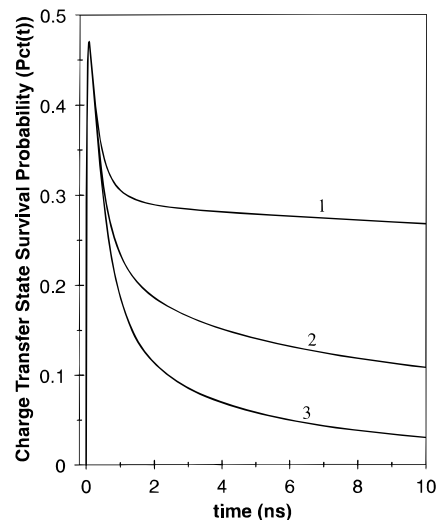


Figure 5. Theoretical charge-transfer survival curves calculated from eq 13 for the same electron-transfer parameters as in Figure 4 but with different Onsager lengths and a diffusion constant of 10 $\text{\AA}^2/\text{ns}$. Curve 1 is for a repulsive potential ($r_c = 60 \text{ \AA}$), while curves 2 and 3 are for no potential ($r_c = 0 \text{ \AA}$) and for an attractive potential ($r_c = -60 \text{ \AA}$), respectively. As can be seen from this figure, the probability of the charge-transfer products surviving is substantially increased by a repulsive Coulombic potential.

slow. Diffusion causes the ions to move into regions where the back transfer is fast.

Figures 3 and 4 were calculated for $r_c = 0$, i.e., for no Coulombic interaction between the ions. However, the charge-transfer-state survival probability depends greatly on the nature of the potential between the products of the forward transfer. Figure 5 illustrates the effects of attraction, repulsion, and no Coulombic potential on the charge-transfer-state survival probabilities for the same set of electron-transfer parameters. For an attractive potential (curve 3), the diffusive motion of the ions is weighted toward approaching the donor, and the probability of back transfer is greatly increased. A repulsive potential, on the other hand (curve 1), can lead to significant ion survival probability, as the acceptor ion is driven preferentially toward the opposite pole from the donor. How far the acceptor ion is driven depends on the micelle radius and Onsager length. For small micelles with low dielectric constants, the acceptor might be driven to the opposite pole from the donor and “trapped” there for some significant fraction of time, since stepping in any direction would then result in an unfavorable increase in Coulombic potential. To study these effects, we used the Monte Carlo simulation to calculate $p(\theta, t)$, the probability that an acceptor ion exists at θ at time t . $p(\theta, t)$ is not an experimental observable. The ion distribution, $p(\theta, t)$, can also be calculated theoretically^{24,40} but requires knowledge of the Green’s function for the two-particle back-transfer problem, i.e., the probability that an acceptor at θ_0 at time 0 would exist as an ion at θ at time t . This Green’s function obeys a differential equation analogous to eq 8 but, because it involves an additional spatial variable, requires a substantial increase in computational time. In the calculation of the experimental observables, $\langle P_{\text{ex}}(t) \rangle$ and $\langle P_{\text{ct}}(t) \rangle$, eqs 7 and 13 afford a great reduction in computational time compared to the Monte Carlo method.

Figure 6 shows the ion distributions as a function of time for Onsager lengths of 0 (no potential—6A), 112 \AA (repulsive potential—6B), and -112 \AA (attraction—6C). The electron-transfer parameters are given in the caption, and $p(\theta, t)$ curves are shown for times of 1, 2, 6, 10, and 15 ns. The total probability of finding an ion at some time t is given by the area under the $p(\theta, t)$ curve for that time. For both the attractive

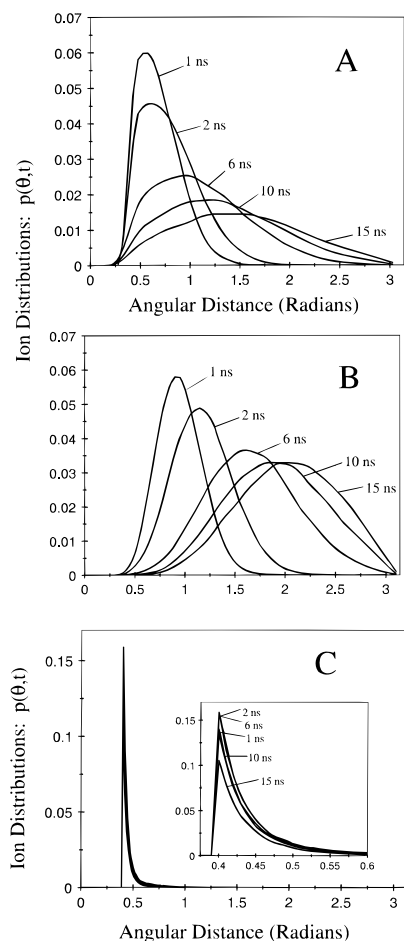


Figure 6. Plots of the charge-transfer acceptor ion distribution for several different times. A is for no Coulombic potential, while B and C are for a repulsive and attractive potential ($r_c = \pm 112 \text{ \AA}$), respectively. Each panel shows the ion distribution at times of 1, 2, 6, 10, and 15 ns. (Time $t = 0$ corresponds to photoexcitation of the donor molecule.) The ion distribution results from the coupling between the forward- and back-transfer dynamics, and the peak of the distribution is heavily influenced by the Coulombic potential. The parameters are $J_f = 50 \text{ cm}^{-1}$, $\beta_f = 1.0 \text{ \AA}^{-1}$, $\Delta G_f = -1.0 \text{ eV}$, $J_b = 400 \text{ cm}^{-1}$, $\beta_b = 1.0 \text{ \AA}^{-1}$, $\Delta G_b = -1.5 \text{ eV}$, $D = 20 \text{ \AA}^2/\text{ns}$, $R = 20 \text{ \AA}$, $N = 9$, $\epsilon_{op} = 2.0$, and $\epsilon_s = 5.0$. The donor–acceptor contact distance was taken to be 8.0 \AA .

potential and the zero potential case, the area under the curves decreases with time as the ion population is depleted by back transfer. In contrast, as Figure 6B shows, a repulsive Coulombic potential results in a large fraction of the charge-transfer ions surviving. The key point to note from the figure, though, is that the peak of the ion distribution changes in a manner consistent with the Coulombic potential. Because the forward transfer is weighted heavily toward short distances, electron transfer occurs preferentially to acceptors near the donor. For an attractive potential, the ions are formed near contact and then are pulled into the donor, where they disappear by back transfer. The inset to Figure 6C shows the short-distance behavior of the ions under the influence of an attractive potential. For all times shown, the distribution is peaked at contact. This occurs because of the fast diffusion constant and steep distance dependence of $k_f(r)$. Although forward transfer may occur to acceptors several angstroms out from contact, the ions formed spend on average very little of their lifetime at these larger distances. The static dielectric constant of 5.0 provides little shielding of the Coulombic potential, and the strong Coulomb force pulls the bulk of the ions in immediately to the contact distance, where they remain until back transfer occurs. Note that for the chosen diffusion constant, $D = 20 \text{ \AA}^2/\text{ns}$, an acceptor

formed even 5 \AA from contact will diffuse in toward the donor in a time approximately equal to $5^2/4D = 300 \text{ ps}$. For forward-transfer rates that peak far out from contact or for systems where the diffusion constant is slower, the ion distribution is observed to move in toward the contact distance over time.

Parts A and B of Figure 6 contrast sharply with part C. In the absence of a Coulombic potential, some of the ions formed near the donor will escape by diffusing across the micelle surface. When the potential is repulsive, the escape probability is greatly enhanced so that the ions become clustered toward the south pole of the micelle by 15 ns. (Note that in Figure 6B, the distribution does not actually peak at $\theta = \pi$, since the $(\sin \theta)/2$ distribution weights the probability toward θ values near the equator.) An ion located at the south pole experiences the minimum potential energy, and any approach to the donor is energetically unfavorable. Thus, for a repulsive potential, long-term escape of the acceptor ion may be possible, and advantageously designed systems could make use of the relatively long ion survival time by reaction with a reagent that is contained in the bulk solvent.

VI. Concluding Remarks

We have presented a theoretical analysis of photoinduced electron transfer with geminate recombination for molecules diffusing on the surface of a micelle. Comparison of the theoretical predictions with Monte Carlo simulations shows perfect agreement, confirming the accuracy of the theory. We have discussed the role of the Coulombic potential and shown the dramatic effect that diffusion has on both the excited-state and charge-transfer-state survival probabilities. This is the first time that forward electron transfer with geminate recombination has been treated for molecules diffusing in a restricted geometry, finite volume system. While these results are for the spherical micelle problem, the method used to obtain them is general and can be applied to any restricted geometry system.

The model system described in section II incorporates several simplifying assumptions. In spite of these assumptions, the theory presented here is valid for a variety of real experimental conditions, provided the donor and micelle concentrations are low. Higher concentrations could result in additional transfer pathways that would need to be incorporated into differential equations (1) and (8) above. The general methods presented here, however, would still apply. Other considerations in applying this theory to real experimental data come from the effects of finite size. Although we have accounted for donor–acceptor excluded volume by limiting the distance of closest approach between the donor and acceptors, we have not included acceptor–acceptor interactions or interactions due to the non-zero size of the micelle surfactant molecules themselves. Also, in calculating the Coulombic potential, we have used an Onsager length determined by a single micelle dielectric constant. The actual potential, however, would have vector components both through the micelle and along the surface, and the dielectric constants could be different in the two directions.

Recently, the roles of solvent structure and hydrodynamic effects have been investigated in the theory for electron transfer in isotropic liquid systems.⁵⁶ This treatment could be extended to the restricted geometry problem by including a distance-dependent form of the diffusion constant and incorporating a pair distribution function in the spatial averaging. Such a pair distribution function would account for the potential, *e.g.*, hard-sphere or Lennard-Jones model, experienced by the donor, acceptors, and micelle surfactant molecules. However, although pair distribution functions in isotropic liquid systems are known, to our knowledge, no similar function has been obtained for

particles on the surface of a sphere. In the absence of analytical expressions, Monte Carlo simulations could possibly be used.

Although the model considered here has the simplifications mentioned above, it should nonetheless be a reasonable first approach to the description of real systems. It includes the most essential features: the distance-dependent forward- and back-electron-transfer rates, the diffusion of the molecules on the micelle surface, the finite number of particles, and the Coulomb interaction between the ions formed by forward electron transfer. Thus, the theory presented here will be useful in the design and analysis of electron-transfer experiments on micelle surfaces, as well as the consideration of possible experiments in other types of restricted geometry systems.

Acknowledgment. Support for this work was provided by the Department of Energy, Office of Basic Energy Sciences (Grant DE-FG03-84ER13251). Partial support of computing equipment was provided by a National Science Foundation departmental grant (Grant NSF-CHE-9408185).

References and Notes

- (1) *J. Phys. Chem.; Rochester Symposium on Charge Transfer in Restricted Geometries* **1991**, 96.
- (2) Fox, M. A. In *Topics in Current Chemistry*; Mattay, J., Ed.; Springer-Verlag: Berlin, 1991; Vol. 159, pp 67.
- (3) Mikhelashvili, M. S.; Michaeli, A. M. *J. Phys. Chem.* **1994**, *98*, 8114.
- (4) Turbeville, W.; Robins, D. S.; Dutta, P. K. *J. Phys. Chem.* **1992**, *96*, 5024.
- (5) Klafter, J.; Drake, J. M.; Levitz, P. *J. Luminesc.* **1990**, *45*, 34.
- (6) Bug, A. L. R.; Grossman, E. L., III; D. D. M.; Berne, B. J. *J. Chem. Phys.* **1992**, *96*, 8840.
- (7) Rabo, J. A.; Gajda, G. J. *Catal. Rev.—Sci. Eng.* **1989–1990**, *31*, 385.
- (8) Bhatia, S.; Beltramini, J.; Do, D. D. *Catal. Rev.—Sci. Eng.* **1989–1990**, *31*, 431.
- (9) Scherzer, J. *Catal. Rev.—Sci. Eng.* **1989**, *31*, 215.
- (10) Zecchina, A.; Arean, C. O. *Catal. Rev.—Sci. Eng.* **1993**, *35*, 261.
- (11) Gaurilidis, A.; Varma, A.; Morbidelli, M. *Catal. Rev.—Sci. Eng.* **1993**, *35*, 399.
- (12) *Photosynthesis*; Hatch, M. D., Boardman, N. K., Ed.; Academic: New York, 1981.
- (13) *Photosynthetic Light Harvesting Systems: Organization and Function*; Scheer, H., Schneider, S., Ed.; W. de Gruyter: Berlin, 1988.
- (14) Guarr, T.; McLendon, G. *Coord. Chem. Rev.* **1985**, *68*, 1.
- (15) Walker, G. C.; Akesson, E.; Johnson, A. E.; Levinger, N. E.; Barbara, P. F. *J. Phys. Chem.* **1992**, *96*, 3728.
- (16) Barbara, P. F.; Walker, G. C.; Smith, T. P. *Science* **1992**, *256*, 975.
- (17) Bixon, M.; Jortner, J.; Cortes, J.; Heitele, H.; Michel-Beyerle, M. E. *J. Phys. Chem.* **1994**, *98*, 7289.
- (18) Akesson, E.; Johnson, A. E.; Levinger, N. E.; Walker, G. C.; DuBrail, T. P.; Barbara, P. F. *J. Chem. Phys.* **1992**, *96*, 7859.
- (19) Asahi, T.; Ohkohchi, M.; Matsusaka, R.; Mataga, N.; Zhang, R. P.; Osuka, A.; Maruyama, K. *J. Am. Chem. Soc.* **1993**, *115*, 5665.
- (20) Cortes, J.; Heitele, H.; Jortner, J. *J. Phys. Chem.* **1994**, *98*, 2527.
- (21) Zeng, Y.; Zimmt, M. B. *J. Phys. Chem.* **1992**, *96*, 8395.
- (22) Fayer, M. D.; Song, L.; Swallen, S. F.; Dorfman, R. C.; Weidemaier, K. In *Ultrafast Dynamics of Chemical Systems*; Simon, J. D., Ed.; Kluwer Academic: Amsterdam, 1994; pp 37.
- (23) Song, L.; Swallen, S. F.; Dorfman, R. C.; Weidemaier, K.; Fayer, M. D. *J. Phys. Chem.* **1993**, *97*, 1374.
- (24) Dorfman, R. C.; Lin, Y.; Fayer, M. D. *J. Phys. Chem.* **1990**, *94*, 8007.
- (25) Murata, S.; Nishimura, M.; Matsuzaki, S. Y.; Tachiya, M. *Chem. Phys. Lett.* **1994**, *219*, 200.
- (26) Murata, S.; Matsuzaki, S. Y.; Tachiya, M. *J. Phys. Chem.* **1995**, *99*, 5354.
- (27) Guarr, T.; McGuire, M. E.; McLendon, G. *J. Am. Chem. Soc.* **1985**, *107*, 5104.
- (28) Eads, D. D.; Dismar, B. G.; Fleming, G. R. *J. Chem. Phys.* **1990**, *93*, 1136.
- (29) Burshtein, A. I. *Chem. Phys. Lett.* **1992**, *194*, 247.
- (30) Burshtein, A. I.; Zharikov, A. A.; Shokhiev, N. V. *J. Chem. Phys.* **1992**, *96*, 1951.
- (31) Lin, Y.; Liu, A.; Trifunac, A. D.; Krongauz, V. V. *Chem. Phys. Lett.* **1992**, *198*, 200.
- (32) Mikhelashvili, M. S.; Feitelson, J.; Dodu, M. *Chem. Phys. Lett.* **1990**, *171*, 575.
- (33) Miller, J. R.; Beitz, J. V.; Huddleston, R. K. *J. Am. Chem. Soc.* **1984**, *106*, 5057.
- (34) Rice, S. A. *Diffusion-Limited Reactions*; Elsevier: Amsterdam, 1985.
- (35) Tachiya, M.; Mozumder, A. *Chem. Phys. Lett.* **1974**, *28*, 87.
- (36) Mikhelashvili, M. S.; Dodu, M. *Phys. Lett. A* **1990**, *146*, 436.
- (37) Dorfman, R. C.; Tachiya, M.; Fayer, M. D. *Chem. Phys. Lett.* **1991**, *179*, 152.
- (38) Weidemaier, K.; Fayer, M. D. *J. Chem. Phys.* **1995**, *102*, 3820.
- (39) Lin, Y.; Dorfman, R. C.; Fayer, M. D. *J. Chem. Phys.* **1989**, *90*, 159.
- (40) Dorfman, R. C. Doctoral Thesis, Stanford University, 1992.
- (41) Marcus, A. H.; Diachun, N. A.; Fayer, M. D. *J. Phys. Chem.* **1992**, *96*, 8930.
- (42) Quitevis, E. L.; Marcus, A. H.; Fayer, M. D. *J. Phys. Chem.* **1993**, *97*, 5762.
- (43) Swallen, S. F.; Fayer, M. D. *J. Chem. Phys.* **1995**, *103*, 8864.
- (44) Swallen, S. F.; Weidemaier, K.; Fayer, M. D. *J. Phys. Chem.* **1995**, *99*, 1856.
- (45) Marcus, R. A. *J. Chem. Phys.* **1956**, *24*, 966.
- (46) Marcus, R. A. *Ann. Rev. Phys. Chem.* **1964**, *15*, 155.
- (47) Agmon, N.; Szabo, A. *J. Chem. Phys.* **1990**, *92*, 5270.
- (48) Finger, K. U.; Marcus, A. H.; Fayer, M. D. *J. Chem. Phys.* **1994**, *100*, 271.
- (49) Press, W. H.; Flannery, B. P.; Teukolsky, S. A.; Vetterling, W. T. *Numerical Recipes in C*; Cambridge University: Cambridge, 1988.
- (50) Pines, E.; Huppert, D.; Agmon, N. *J. Chem. Phys.* **1988**, *88*, 5620.
- (51) Agmon, N.; Hopfield, J. J. *J. Chem. Phys.* **1983**, *78*, 6947.
- (52) Valleau, J. P.; Whittington, S. G. In *Statistical Mechanics*; Berne, B. J., Ed.; Plenum: New York, 1977; Vol. 5.
- (53) Allen, M. P.; Tildesley, D. J. *Computer Simulation of Liquids*; Clarendon: Oxford, 1987.
- (54) Chanon, M.; Hawley, M. D.; Fox, M. A. In *Photoinduced Electron Transfer, Part A*; Fox, M. A., Chanon, M., Eds.; Elsevier: Amsterdam, 1988; p 10.
- (55) Meites, L.; Zuman, P.; Scott, W. J., et al. *CRC Handbook Series in Organic Electrochemistry*; CRC: Cleveland, OH, 1977; Vol. 1.
- (56) Swallen, S. F.; Weidemaier, K.; Fayer, M. D. *J. Chem. Phys.*, in press.

JP952724G